FULL PAPER

Dalton
www.rsc.org/dalton

# Preparation of stable $AsBr_4^+$ and $I_2As–PI_3^+$ salts. Why didn't we succeed to prepare $AsI_4^+$ and $As_2X_5^+$? A combined experimental and theoretical study†

**Marcin Gonsior**[a] **and Ingo Krossing***[b]

[a] *Universität Karlsruhe, Institut für Anorganische Chemie, Engesserstr. Geb. 30.45, 76128, Karlsruhe, Germany. E-mail: marcin.gonsior@chemie.uni-karlsruhe.de*

[b] *Ecole Polytechnique Fédérale de Lausanne (EPFL), Laboratory of Inorganic and Coordination Chemistry (LCIC), ISIC-BCH, 1015, Lausanne, Switzerland. E-mail: ingo.krossing@epfl.ch*

***Received 22nd November 2004, Accepted 16th February 2005***
***First published as an Advance Article on the web 2nd March 2005***

In analogy to our successful "$PX_2^+$" insertion reactions, an "$AsX_2^+$" insertion route was explored to obtain new arsenic halogen cations. Two new salts were prepared: $AsBr_4^+[Al(OR)_4]^-$, starting from $AsBr_3$, $Br_2$ and $Ag[Al(OR)_4]$, and $I_2As–PI_3^+[Al(OR)]_4$ from $AsI_3$, $PI_3$ and $Ag[Al(OR)_4]$ ($R = C(CF_3)_3$). The first cation is formally a product of an "$AsBr_2^+$" insertion into the $Br_2$ molecule and the latter clearly a "$PI_2^+$" insertion into the As–I bond of the $AsI_3$ molecule. Both compounds were characterized by IR and NMR spectroscopy, the first also by its X-ray structure. Reactions of $Ag[Al(OR)_4]$ with $AsI_3$ do not lead to ionization and AgI formation but rather lead to a marginally stable $Ag(AsI_3)_2^+[Al(OR)]_4$ salt. Despite many attempts we failed to prepare other PX-cation analogues such as $AsI_4^+$, $As_2X_5^+$ and $P_4AsX_2^+$ (X = Br, I). To explain these negative results the thermodynamics of the formation of $EX_2^+$, $EX_4^+$ and $E_2X_5^+$ (E = As, P; X = Br, I) was carefully analyzed with MP2/TZVPP calculations and inclusion of entropy and solvation effects. We show that $As_2Br_5^+$ is in very rapid equilibrium with $AsBr_2^+$ and $AsBr_3$ ($\Delta G^\circ_{(CH_2Cl_2)} = +30$ kJ mol$^{-1}$). The extremely reactive $AsBr_2^+$ cation available in the equilibrium accounts for the observed decomposition of the $[Al(OR)_4]^-$ anion. By contrast, the stability of $AsI_3$ against $Ag[Al(OR)_4]$ appears to be kinetic and, if prepared by a suitable route, $As_2I_5^+$ would be expected to have a stability intermediate between the known $P_2I_5^+$ and $P_2Br_5^+$.

## Introduction

Few reports on binary As–X species (X = halogen) have appeared and binary As–X cations with more than one arsenic atom are unknown. The limited spectrum of well characterized binary As–X neutrals ranges from $AsF_5$,[1,2] very unstable $AsCl_5$ (decomposition above −50 °C),[3–7] and $AsCl_nF_{5-n}$ ($n$ = 1–4)[8–12] to $AsX_3$ (X = F, Cl, Br, I) and easily decomposing $As_2I_4$.[13] These rare examples may be contrasted by the wide range of phosphorus halides known: $PX_5$ (X = F, Cl, Br),[13,14] $PX_3$ (X = F, Cl, Br, I),[13] $P_2X_4$ (X = F, Cl, Br, I),[13,15] $P_6X_6$,[16] $P_3I_5$,[17] $P_4X_2$ (X = Br, Cl)[15] and $P_7X_3$ (X = Br, I).[15] Turning to the cations, the situation is similar: while several salts of $PCl_4^+$, $PBr_4^+$ and $PI_4^+$ are well characterized by X-ray, $^{31}$P NMR and vibrational spectroscopy as well as quantum-chemical calculations[18–25] ($PF_4^+$ was observed by Raman spectroscopy),[26,27] the $AsX_4^+$ cations characterized by an X-ray structure are limited to $AsCl_4^+AsF_6^-$,[28] $AsCl_4^+[As(OTeF_5)_6]^-$ and $AsBr_4^+[As(F)(OTeF_5)_5]^-$.[29] The nature of $AsI_4^+$ and $AsF_4^+$ is somewhat questionable; these cations are reported to be highly unstable salts decomposing above −78 °C and were described by Raman and IR spectroscopy.[30,31] The only other binary As–X cations known are of type $AsX_2^+$ ($As^{III}$) and were observed in a mass spectrometer.[32,33] Other As–X cations such as the As analogues of the low valent phosphorus cations $P_2X_5^+$ (X = Br, I),[24,34] $P_3I_6^+$,[25,35] or phosphorus rich $P_5X_2^+$ (X = Cl, Br, I)[25,35,36] still remain unknown in arsenic chemistry.

A new method to prepare hitherto unknown binary phosphorus halogen cations is the insertion of a "$PX_2^+$" intermediate—a positively charged carbene analogue—into the P–P or P–X (X = Br, I) bonds of neutral $P_nX_y$ molecules forming the species mentioned above. The "$PX_2^+$" cation is a short lived intermediate generated *in situ* from phosphorus trihalide and the silver salt $Ag[Al(OR)_4]$ ($R = C(CF_3)_3$) (see Scheme 1).[37–40]

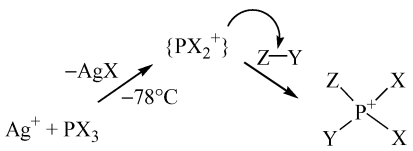


**Scheme 1** Formation of the "$PX_2^+$" intermediate and its insertion into the Z–Y bond of a simple molecule (*e.g.* $I_2P–I$, Br–Br, $PI_2–PI_2$ *etc.*).

Insertion of the $PX_2^+$ cation (X = Cl, Br, I) into the Z–Y bond of simple molecules with Z = Br, I, P or S and Y = Br, I, P led to several new binary and ternary P–X cations in good yields.[24,25,35,41] This carbenoid $PX_2^+$ cation is highly reactive and the above insertion reactions require a robust counterion to avoid decomposition. The only Weakly Coordinating Anion (WCA) that was compatible with the cations, was the fluorinated alkoxyaluminate $[Al(OR)_4]^-$ with $R = C(CF_3)_3$.[36,37,39] For a comparison of the stabilities of several WCAs see our earlier work.[42,43] The intermediately generated "$PX_2^+$" cation does not decompose this anion at low temperature (−78 to −30 °C) and the insertion products are stable with those anions in solution between −30 and 0 °C (some even for 15 min at RT). Therefore, we were interested to transfer this pathway to arsenic chemistry. Thus, using an "$AsX_2^+$" intermediate generated *in situ* from $AsX_3$ (X = Br, I) and $Ag[Al(OR)_4]$, it should be possible to synthesize this class of compounds by insertion reactions (see Fig. 1 for target cations).

However, the transfer of this insertion methodology from P to As turned out to be rather difficult and the only compounds that could be synthesized by this route were $AsBr_4^+[Al(OR)_4]^-$ and $I_2AsPI_3^+[Al(OR)_4]^-$. In this contribution we describe successful and unsuccessful synthetic efforts directed to the preparation of

† Electronic supplementary information (ESI) available: Detailed experimental and theoretical discussion. See http://www.rsc.org/suppdata/dt/b4/b417629d/

DOI: 10.1039/b417629d

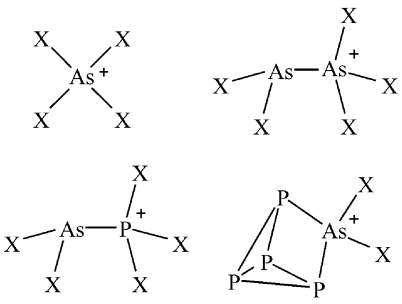

X = Br, I

**Fig. 1** Arsenic and arsenic–phosphorus halogen cations that were targeted by insertion of "$AsX_2^+$" into the X–X, E–X and P–P bonds of $X_2$, $EX_3$ and $P_4$ (E = P, As; X = Br, I).

new binary As–X cations and analyze the reasons for the failure with the additional help of detailed *ab initio* calculations.

## Results

Due to the at first sight rather confusing experimental results, we start with the general thermochemistry underlying the proposed reactions leading to the products as in Fig. 1.

### Initial thermodynamic calculations

A word of caution before starting: The thermodynamics of a reaction may be predicted by quantum chemical calculations. However, the underlying kinetics is not assessed by this approach. Thus experiments are needed to verify the predictions made based on the computed thermodynamics. Since earlier work[24,35] showed the necessity to employ *ab initio* and not DFT methods, we exclusively used the balanced MP2/TZVPP level[44–46] throughout the work. Energies and geometries of the binary P–X cations obtained with this level are in very good agreement with the experiment and thus lend confidence to conclusions drawn from these calculations. All enthalpies and free energies given in this section include the ZPEs, entropic and thermal contributions to the free energy at 298 K as well as the solvation energies (in $CH_2Cl_2$ using the COSMO solvation model[47]).

**Thermodynamics of the formation of $E_2X_5^+$ and $EX_4^+$ (E = P, As).** We assessed the enthalpies for the formation of the "$EX_2^+$" intermediate and $EX_4^+$ or $E_2X_5^+$ starting from the elemental trihalide, dihalogen and the in $CH_2Cl_2$ solution prevailing $Ag(CH_2Cl_2)_3^+$ cation (see Table 1).

Excluding the formation of solid AgX, the energetics of the formation of all arsenic cations, the $PX_2^+$ intermediate and $P_2Br_5^+$ are endergonic in solution. However, as shown experimentally, $PX_2^+$ formation proceeds even at −78 °C.[24,25,35] In agreement with this, all reactions are exergonic, if the formation of solid AgX is assumed. Overall, the solution Gibbs energies for the formation of $PX_4^+$ and $P_2X_5^+$ are by 35–65 kJ mol$^{-1}$ more favorable than those for $AsX_4^+$ and $As_2X_5^+$, but, when including the formation of solid AgX, also the arsenic cations should form.

### Syntheses

All experiments were started at −78 °C to avoid anion decomposition by *in situ* formed "$AsX_2^+$". Than the mixtures were allowed to warm to about −30 °C, or, if no AgX precipitation was observed, also warmed to ambient temperature. In the following R denotes the $C(CF_3)_3$ group.

**Reactions of $AsX_3$ and $Ag[Al(OR)_4]$.** We attempted to generate the $AsX_2^+$ intermediate according to eqn. (7).

$$AsX_3 + Ag[Al(OR)_4] \rightarrow AsX_2^+[Al(OR)_4]^- + AgX\ (X = Br, I) \quad (7)$$

For $AsBr_3$, precipitation of AgBr was observed and after removing all volatiles of the mixture the weight of the reaction residue was reduced to about a half, typical for anion decomposition (also NMR). Solid $AsBr_3$ and solid $Ag[Al(OR)_4]$ ground in the glove box for 15 min react already in the solid state at room temperature and decompose the anion (mass balance, IR, NMR). From this solid-state reaction (after dissolving the residue in THF–$CH_2Cl_2$ mixture) the decomposition product $[(RO)_2AlF(THF)]_2$ was isolated and completely characterized (X-ray, IR, NMR). By contrast, $AsI_3$ did not react under the same conditions.

The synthesis of $As_2X_5^+$ salts was attempted according to eqn. (8):

$$2AsX_3 + Ag[Al(OR)_4] \rightarrow As_2X_5^+[Al(OR)_4]^- + AgX\ (X = Br, I) \quad (8)$$

No visible reaction occurred below −30 °C. Rising the temperature to −20 °C led to precipitation of AgBr but only the decomposition of the anion was observed (IR, NMR, mass balance). In all those experiments with $AsBr_3$, the only crystalline material that we isolated was $AsBr_3$ (unit cell determination, IR).

When 1 or 2 equiv. of $AsI_3$ were reacted with $Ag[Al(OR)_4]$ no reaction was observed even at room temperature. No precipitation of AgI occurred even when we changed the solvent to a $CS_2$–$CH_2Cl_2$ mixture to improve the solubility of $AsI_3$. The reaction mixture left at room temperature for weeks in a sealed NMR tube showed no decomposition of the anion and still no precipitation of AgI. From cooled $AsI_3$/$Ag[Al(OR)_4]$ mixtures only $AsI_3$ precipitated. We never had any indication for the precipitation of $Ag(AsI_3)_X^+[Al(OR)_4]^-$ salts, although they may be present in solution. This may be concluded from the essentially better solubility of $AsI_3$ in $Ag[Al(OR)_4]$–$CH_2Cl_2$ solution than in pure $CH_2Cl_2$ and the intense red color of the solution. Pure $AsI_3$ is nearly insoluble in $CH_2Cl_2$ and the solution is only little colored. Interestingly, the IR-spectra of the solid-state reaction of 2 equiv. $AsI_3$ and the "naked" silver salt ground in the glove-box for 15 min showed that $AsI_3$ molecules

**Table 1** $\Delta H^\circ_{(g)}$, $\Delta G^\circ_{(g)}$, $\Delta G^\circ_{(CH_2Cl_2)}$ for the formation of $EX_4^+$ and $E_2X_5^+$. The values in parenthesis in italics include the formation of solid AgX.[48]

| | Eqn. | Reaction (MP2/TZVPP) | $\Delta H^\circ_{(g)}$ | $\Delta G^\circ_{(g)}$ | $\Delta G^\circ_{(CH_2Cl_2)}$ |
|---|---|---|---|---|---|
| | (1a) | $AsBr_3 + Ag(CH_2Cl_2)_3^+ \rightarrow AsBr_2^+ + AgBr + 3CH_2Cl_2$ | +378 | +244 | +130 (*−87*) |
| | (1b) | $AsI_3 + Ag(CH_2Cl_2)_3^+ \rightarrow AsI_2^+ + AgI + 3CH_2Cl_2$ | +329 | +196 | +101 (*−96*) |
| | (2a) | $AsBr_3 + Br_2 + Ag(CH_2Cl_2)_3^+ \rightarrow AsBr_4^+ + AgBr + 3CH_2Cl_2$ | +158 | +79 | +14 (*−203*) |
| | (2b) | $AsI_3 + I_2 + Ag(CH_2Cl_2)_3^+ \rightarrow AsI_4^+ + AgI + 3CH_2Cl_2$ | +143 | +67 | +12 (*−185*) |
| | (3a) | $2AsBr_3 + Ag(CH_2Cl_2)_3^+ \rightarrow As_2Br_5^+ + AgBr + 3CH_2Cl_2$ | +235 | +155 | +101 (*−116*) |
| | (3b) | $2AsI_3 + Ag(CH_2Cl_2)_3^+ \rightarrow As_2I_5^+ + AgI + 3CH_2Cl_2$ | +151 | +72 | +30 (*−167*) |
| | (4a) | $PBr_3 + Ag(CH_2Cl_2)_3^+ \rightarrow PBr_2^+ + AgBr + 3CH_2Cl_2$ | +378 | +243 | +130 (*−87*) |
| | (4b) | $PI_3 + Ag(CH_2Cl_2)_3^+ \rightarrow PI_2^+ + AgI + 3CH_2Cl_2$ | +329 | +198 | +104 (*−93*) |
| | (5a) | $PBr_3 + Br_2 + Ag(CH_2Cl_2)_3^+ \rightarrow PBr_4^+ + AgBr + 3CH_2Cl_2$ | +97 | +21 | −49 (*−266*) |
| | (5b) | $PI_3 + I_2 + Ag(CH_2Cl_2)_3^+ \rightarrow PI_4^+ + AgI + 3CH_2Cl_2$ | +107 | +36 | −18 (*−215*) |
| | (6a) | $2PBr_3 + Ag(CH_2Cl_2)_3^+ \rightarrow P_2Br_5^+ + AgBr + 3CH_2Cl_2$ | +181 | +106 | +48 (*−169*) |
| | (6b) | $2PI_3 + Ag(CH_2Cl_2)_3^+ \rightarrow P_2I_5^+ + AgI + 3CH_2Cl_2$ | +107 | +37 | −6 (*−191*) |

coordinate to the $Ag^+$ cation. In this reaction the anion was not decomposed unlike in the solid-state reaction between $AsI_3$, $I_2$ and $Ag[Al(OR)_4]$ (see below) and $Ag(AsI_3)_x^+[Al(OR)_4]^-$ with $x$ likely to be 2 formed.

**The reaction of $AsBr_3$, $P_4$ and $Ag[Al(OR)_4]$.** In a reaction analogously to the synthesis of $P_5X_2^+$ (X = Br, I) we reacted $AsBr_3$, $P_4$ and $Ag[Al(OR)_4]$ to obtain $P_4AsBr_2^+[Al(OR)_4]^-$ (eqn. (9)).

$$P_4 + AsBr_3 + Ag[Al(OR)_4] \rightarrow P_4AsBr_2^+[Al(OR)_4]^- + AgBr \quad (9)$$

The "$AsBr_2^+$" intermediate was anticipated to react with $P_4$ to the $P_4AsBr_2^+$ salt. However, after precipitation of AgBr above −30 °C only decomposition of the anion without noticeable degradation of white phosphorus was observed. In the $^{31}P$ NMR only the signal of dissolved $Ag(P_4)x^+$ ($x = 1, 2$) was visible. This is similar to our earlier reaction of $PCl_3$, $P_4$ and $Ag[Al(OR)_4]$ that led to $Ag(P_4)_2^+[(RO)_3Al–F–Al(OR)_3]^-$.[36]

**The reaction of $AsI_3$, $PI_3$ and $Ag[Al(OR)_4]$.** After the unsuccessful experiments with $AsI_3$ we carried out the reaction between $AsI_3$, $PI_3$ and $Ag[Al(OR)_4]$ to obtain the mixed $AsPI_5^+$ cation (eqn. (10)).

$$AsI_3 + PI_3 + Ag[Al(OR)_4] \rightarrow AsPI_5^+[Al(OR)_4]^- + AgI \quad (10)$$

In the $^{31}P$ NMR spectra of the reaction mixture (243 K, in $CD_2Cl_2$), two groups of signals were found: one that was assigned to the $P_2I_5^+$ cation—the known product of a $PI_2^+$ insertion into the P–I bond of $PI_3$ and another which we assign to the $I_2As–PI_3^+$ cation. Considering that $AsI_3$ does not react with $Ag[Al(OR)_4]$, the $AsI_2PI_3^+$ cation is the only likely product of a $PI_2^+$ insertion (except $P_2I_5^+$, eqn. (11)).

$$\begin{array}{ccc} & Ag^+ + PI_3 & \\ & \downarrow -AgI & \\ I_2As–PI_3^+ & \xleftarrow{I_2As–I} \quad PI_2^+ \quad \xrightarrow{I–PI_2} & I_2P–PI_3^+ \end{array} \quad (11)$$

The intensities of the signals of both cations in the $^{31}P$ NMR are 1 : 1. Neither addition of $CS_2$ (to dissolve more $AsI_3$) nor additional $AsI_3$ (1 equiv.) changed the product ratio. Another reaction with 6 equiv. of $AsI_3$, 1 equiv. of $PI_3$ and the silver salt was performed in $CH_2Cl_2–CS_2$ (3 : 1) mixture for improved solubility of $AsI_3$. Again the product ratio was the same and we could not isolate a pure $I_2As–PI_3^+$ salt from the reaction mixture. However, we succeeded to characterize $I_2As–PI_3^+[Al(OR)_4]^-$ as a mixture with $P_2I_5^+$ also by IR spectroscopy.

**Reactions of $AsX_3$, $X_2$ and $Ag[Al(OR)_4]$. Successful preparation of $AsBr_4^+[Al(OR)_4]^-$.** The reactions according to eqn. (12) were carried out at −78 °C and kept below −30 °C.

$$AsX_3 + X_2 + Ag[Al(OR)_4] \rightarrow AsX_4^+[Al(OR)_4]^- + AgX \ (X = Br, I) \quad (12)$$

However, only the preparation of $AsBr_4^+[Al(OR)_4]^-$ proceeded as indicated in eqn. (12). After precipitation of AgBr and low-temperature work-up we isolated slightly yellowish crystals in 54% yield. A X-ray single crystal structure determination showed the crystals to be $AsBr_4^+[Al(OR)_4]^-$ (**1**). The salt **1** was also characterized by IR spectroscopy and by $^{75}As$ NMR.

In the attempted $AsI_4^+$ synthesis, precipitation of yellow AgI was not observed below −30 °C but only voluminous dark solids precipitated at −78 °C. These solids could be reversibly dissolved between −50 and −30 °C. We suspect that the precipitated solids consist of a complex $Ag(I_2)x^+$ salt, since very recently it was found that the silver cation forms stable adducts with iodine given the right counterion (see $Ag(I_2)^+[AsF_6]^-$).[49] $AsI_3$ is almost insoluble in $CH_2Cl_2$ at low temperature and due to the volume and shape of the precipitate, solid $I_2$ could also be excluded. Warming the reaction mixture above 0 °C led to formation of AgI but also to a complete decomposition of the anion ($^{13}C$, $^{19}F$ NMR, mass balance)—presumably due to the reaction of iodine and the silver salt (see below, eqns. (13) and (14)). No single crystals could be isolated, except those of $AsI_3$ which were always isolated from the non-volatile residue of this reaction (Raman, IR, X-ray).

To exclude solvent effects, the solid-state reaction between $AsI_3$, $I_2$ and $Ag[Al(OR)_4]$ was carried out in the glove box. However, only decomposition of the anion occurred (IR).

To confirm that the reaction between $I_2$ and $Ag^+$ leads to anion decomposition (see eqns. (13) and (14)) we reacted $I_2$ and $Ag[Al(OR)_4]$ at room temperature and observed complete decomposition of the anion after precipitation of AgI.

$$I_2 + Ag^+ \rightarrow "I^+" + AgI \quad (13)$$

$$"I^+" + [Al(OR)_4]^- \rightarrow \text{decomposition} \quad (14)$$

"$I^+$" in eqns. (13) and (14) denote the hypothetical species formed from $I_2$ and $Ag^+$ upon precipitation of the silver iodide.

## Crystal structures

**Crystal structure of $AsBr_4^+[Al(OR)_4]^-$.** The air- and moisture-sensitive yellowish block-shaped crystals of **1** were grown from a concentrated $CH_2Cl_2$ solution at −80 °C.

The cation in **1** (Fig. 2) forms an almost ideal tetrahedron with Br–As–Br angles between 108.93(2) and 110.54(2)°, on average 109.47(2)°. The As–Br bond lengths range from 2.2144(5) to 2.2318(5) Å and are 2.2257(5) Å on average. The $[Al(OR)_4]^-$ anion has the usual geometry.[50] This is the second structural report of the $AsBr_4^+$ cation. The As–Br distances in **1** are in good agreement with the previously characterized $AsBr_4^+[As(F)(OTeF_5)_5]^-$ (2.225(2)–2.236(2) Å, average 2.232(2) Å)[29] and our quantum chemically calculated value of the As–Br distance of 2.231 Å (MP2/TZVPP). There is only one weak, As1 ··· F1 contact at 3.552 Å longer than the van der Waals limit (sum of van der Waals radii 3.5 Å), but each of the bromine atoms exhibits at least one shorter fluorine contact, *i.e.* Br1 3.223 Å, Br2 3.254 Å, Br3 3.098 Å, while Br4 has two close contacts at 3.237 and 3.266 Å (sum of van der Waals radii of Br and F = 3.4 Å). In total 17 weak Br–F contacts are formed (see Fig. 3 and Table A, ESI†).

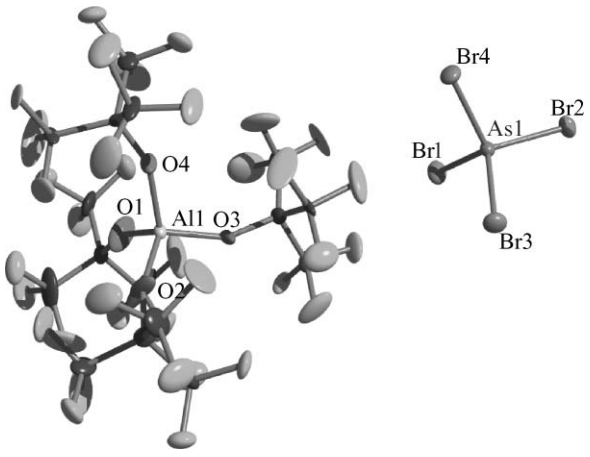


**Fig. 2** Section of the solid-state structure of $AsBr_4^+[Al(OR)_4]^-$. Thermal ellipsoids were drawn at the 25% probability level. Selected bond lengths (Å) and angles (°): As1–Br1 2.2318(5), As1–Br2 2.2284(4), As1–Br3 2.2144(5), As1–Br4 2.2283(4), Al1–O1 1.664(2), Al1–O2 1.679(2), Al1–O3 1.7030(9), Al1–O4 1.7039(9); Br3–As1–Br2 109.02(2), Br3–As1–Br4 108.93(2), Br2–As1–Br4 110.54(2), Br3–As1–Br1 109.43(2), Br2–As1–Br1 109.64(2), Br4–As1–Br1 109.27(2).

The multitude of Br ··· F contacts suggests that the charge is distributed equally over the four bromine atoms. Similar to the $AsBr_4^+[As(F)(OTeF_5)_5]^-$ crystal structure there are no substantial $Br_4As^+ \cdots F$ interactions. In contrast, in

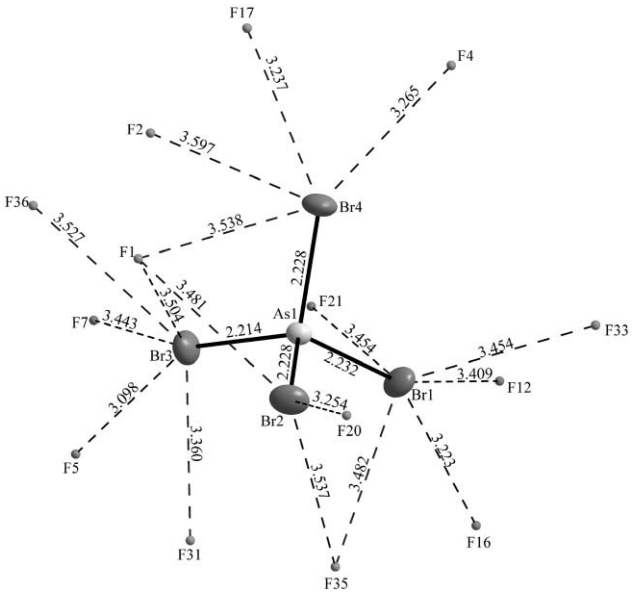


**Fig. 3** Weak fluorine contacts of the $AsBr_4^+$ cation in **1**. The F–Br contacts are shown within the sum of van der Waals radii of 3.4 Å with a tolerance of +5%. Thermal ellipsoids were drawn at the 25% probability level.

$AsCl_4^+[As(OTeF_5)_6]^-$ several closer $Cl_4As^+ \cdots F$ contacts were found (from 3.377 to 3.432 Å).[29] In the solid state, the salt **1** forms a distorted CsCl structure with the almost spherical $[Al(OR)_4]^-$ anion forming a distorted primitive cubic array and the $AsBr_4^+$ cations residing in the center of the cubic interstices (Fig. 4).

**Crystal structure of $[(RO)_2Al(\mu\text{-}F)(THF)]_2$.** Colorless plates of $[(RO)_2Al(\mu\text{-}F)(THF)]_2$ were grown from a $CH_2Cl_2$–THF solution at −28 °C. Neutral $[(RO)_2Al(\mu\text{-}F)(THF)]_2$ is a dimer, which forms a centrosymmetric planar four-membered $Al_2F_2$ ring as the central structural building block. The aluminium atom in every $(RO)_2Al(\mu\text{-}F)(THF)$ unit has a five-fold coordination in between a square pyramid and a trigonal bipyramid (Figs. 5 and 6).

Similar building blocks were earlier found in $[(R'OH)Tl][Al(OR')_3F]_2$[51] (R′ = $C(H)(CF_3)_2$) or $[PhC(CH(SiMe_3)_2)N(SiMe_3)AlF_2]_2$[52] and $[(R'O)(Me)Al(OR')_2AlF(Me)]_2$[53] (R′ = 2,6-i-$Pr_2C_6H_3$). There are two sets of Al–F distances in $[(RO)_2AlF(THF)]_2$: 1.791(1) and 1.887(1) Å which may be compared to the Al–F distances in ionic $[(R'OH)Tl][Al(OR')_3F]_2$ (1.839(6) and 1.919(6) Å),[51] in neutral $[PhC(C(SiMe_3)_2)N(SiMe_3)AlF_2]_2$ (1.829(3) and 1.850(3) Å) and $[(R'O)(Me)Al(OR')_2AlF(Me)]_2$ (1.812(2) and 1.879(2) Å). The Al–$O_{THF}$ dative bond (1.895(1) Å) in $[(RO)_2AlF(THF)]_2$ is longer than Al–$O_{THF}$ (1.826(2) Å) in the Lewis acid–base adduct $(THF)\cdot Al(OR)_3$.[36]

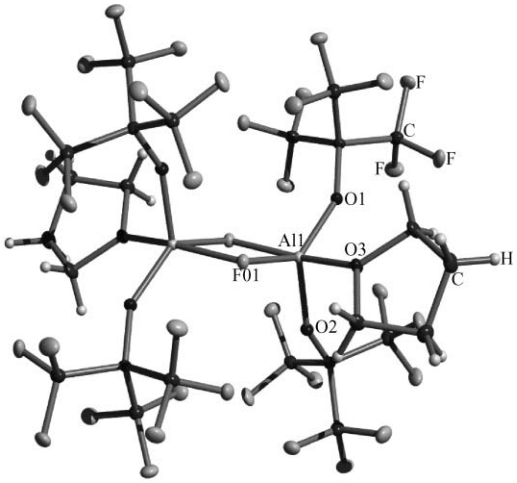


**Fig. 5** Solid $[(RO)_2Al(\mu\text{-}F)(THF)]_2$ with 25% probability ellipsoids.

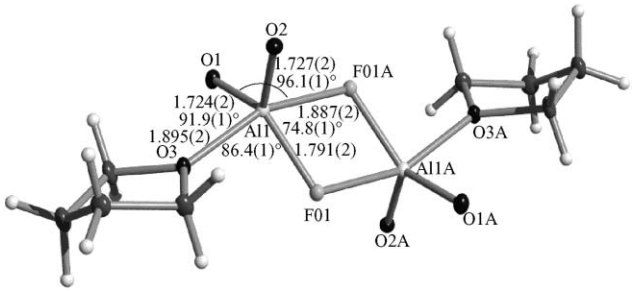


**Fig. 6** The core of the solid-state structure of $[(RO)_2Al(\mu\text{-}F)(THF)]_2$. All the $-C(CF_3)_3$ groups were omitted for clarity. Thermal ellipsoids (except for isotropic H) were drawn at the 25% probability level.

## NMR and vibrational spectroscopy

**$^{75}As$ NMR of $AsBr_4^+[Al(OR)_4]^-$.** Since $^{75}As$ is a quadrupolar nucleus ($I$ = 3/2, 100% abundance), only species with a high local symmetry can be expected to give signals in the $^{75}As$ NMR spectrum. We recorded a spectrum of freshly prepared **1** in a NMR tube reaction in $CD_2Cl_2$ solvent (according to eqn. (12), X = Br). At −65 °C a singlet appeared at $\delta$ −148.2 (s, $\nu_{1/2}$ = 983.2 Hz) which is assigned to the $AsBr_4^+$ cation (Fig. C. ESI†). This chemical shift is in agreement with the experimental value of $AsBr_4^+[AsF(OTeF_5)_5]^-$ (−134.3 ppm in $SO_2ClF$ at r.t.) recorded by Schrobilgen *et al.*[29]

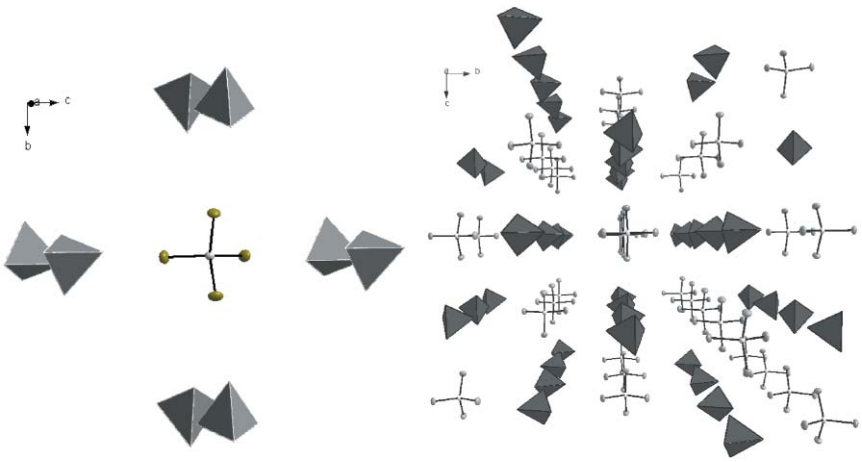

**Fig. 4** Distorted cubic primitive packing of the ions in $AsBr_4^+[Al(OR)_4]^-$. The $AsBr_4^+$ cation is surrounded by eight $[Al(OR)_4]^-$ anions forming a distorted cubic coordination sphere. All R groups were omitted for clarity. The $AlO_4$ units are shown as tetrahedra.

**IR spectrum of $AsBr_4^+[Al(OR)_4]^-$.** The IR spectrum of crystalline **1** recorded in Nujol (Fig. 7) shows, apart from the anion bands, an intense absorption at 354 $cm^{-1}$: the $T_2$ mode of $AsBr_4^+$. All other bands are due to the anion (no unassigned vibration, Table F, ESI†).

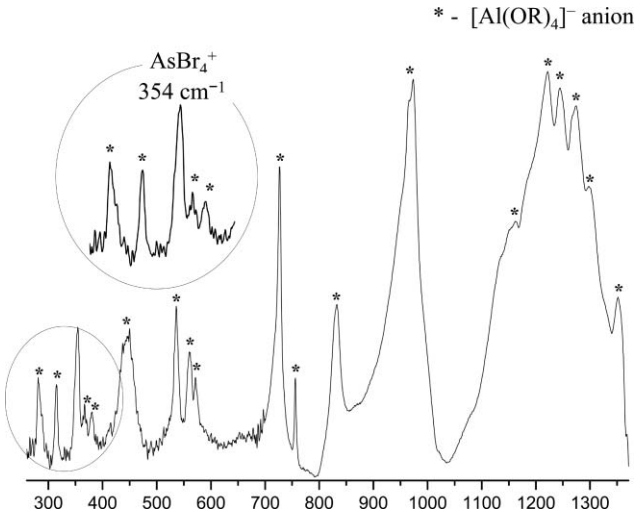


**Fig. 7** IR spectrum of a Nujol mull of crystalline **1** showing the $T_2$ vibration of $AsBr_4^+$ cation at 354 $cm^{-1}$. The anion vibrations are marked by an asterisk.

This result is in very good agreement with the calculated 378 $cm^{-1}$ value at the MP2/TZVPP and 337 $cm^{-1}$ value at the BP86/SV(P) level. The $\nu(T_2)$ in the Raman spectrum of $AsBr_4^+[AsF(OTeF_5)_5]^-$ was reported at 353 $cm^{-1}$.[29] In $AsBr_4^+AsF_6^-$ this vibration was found at 349 $cm^{-1}$ (Raman spectrum).[54,55] It may be noted that $\nu(T_2)$ increases with decreasing coordination power of the anion, *i.e.*: $\nu(T_2, [AsF_6]^-) < \nu(T_2, [FAs(OTeF_5)_5]^-) < \nu(T_2, [Al(OR)_4]^-)$ or 349 < 353 < 354 $cm^{-1}$.

**$^{31}P$ NMR spectrum of $I_2As–PI_3^+$.** The $^{31}P$ NMR spectrum of the $AsI_2PI_3^+/P_2I_5^+$ salt mixture was recorded at −80 °C over a period of one month (Fig. 8).

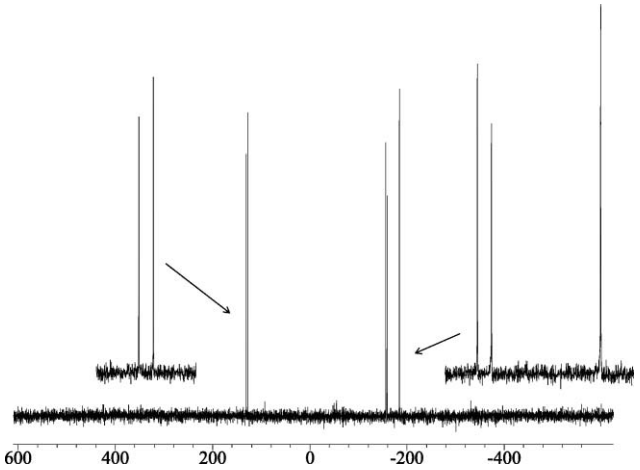


**Fig. 8** $^{31}P$ NMR spectrum of the products of the reaction between $PI_3$, $AsI_3$ and $Ag[Al(OR)_4]$ (eqn. (10)). In the range from +600 to −600 ppm only signals of $P_2I_5^+$ (two doublets) and $I_2As–PI_3^+$ (s) are observed. The spectrum was recorded at −80 °C.

No anion decomposition was visible when the sample was stored at −28 °C. Two groups of signals were found: the $P_2I_5^+$ cation was observed at $\delta(^{31}P)$ +129.7 (doublet of the $I_2P–$ moiety, $^1J_{PP}$ = 325.1 Hz) and at $\delta(^{31}P)$ −157.2 (doublet of $–PI_3^+$, $^1J_{PP}$ = 325.1 Hz) which is in good agreement with earlier data.[24] Another broader signal (see Fig. 8) we assign to the $–PI_3^+$ moiety in $I_2As–PI_3^+$ appeared at $\delta(^{31}P)$ −183.6 (no coupling to As was observed). The $^{31}P$ chemical shift of **2** at −183.6 ppm is close to the phosphonium resonance of the $–PI_3^+$ moiety in $P_2I_5^+$ at $\delta(^{31}P)$ −157.2. The similarity of the chemical shifts suggests an "exchange" of the $I_2P–$ substituent in $I_2P–PI_3^+$ against $I_2As–X$ giving the $I_2As–PI_3^+$ cation. The integration of the signals showed the ratio $P_2I_5^+$ : $AsI_2PI_3^+$ to be 1 : 1.

**IR spectrum of $I_2As–PI_3^+$.** The IR spectra of the mixture of $I_2As–PI_3^+$ and $P_2I_5^+$ cations were recorded in Nujol between CsI plates. The isolation of pure **2** from the reaction mixture failed. However, we could assign all bands of $I_2As–PI_3^+$ in a microcrystalline fraction (I) and fraction (II), that resulted from removing the solvent of the reaction residue (see Fig. B and section, ESI†). It should be noted that vibrations at 635 and 864 $cm^{-1}$ indicate partial decomposition of the anion ($[(RO)_3Al–F–Al(OR)_3]^-$ formation[36]). All attempts to obtain a Raman spectrum of fraction I/II failed due to immediate decomposition in the laser beam. The frequency calculation performed at the MP2/TZVPP level for **2** is in good agreement with our assignments in Table 2. For more details, the interested reader is referred to a deposited section.

## Computational results

All the species present in this paper were calculated at the MP2/TZVPP level with the exception of molecules participating in the ligand abstraction reaction according to eqn. (15). Due to their size, $EX_2OR$ (E = As, P; X = Br, I), $Al(OR)_3$ and $Al(OR)_4^-$ (R = $C(CF_3)_3$) were only calculated at the BP86/SVP level.

**Binary and ternary P/As/X cations.** The BP86/SVP level gave unsatisfying results for the $As_2X_5^+$ cations. Neither an appropriate As–As distance, *i.e.* in $As_2Br_5^+$ 2.701 Å and in $As_2I_5^+$ 2.675 Å at the BP86/SVP level (*cf.* MP2 geometries of the $As_2X_5^+$ cations in Fig. 9), nor a true minimum could be reached (the optimized $As_2Br_5^+$ structure always had one imaginary frequency). Similar results and the failure of DFT has been reported for the lighter homologous binary P–X cations. In contrast, the MP2/TZVPP calculated As–As distances in $As_2X_5^+$ (X = Br, I), 2.493 and 2.472 Å, are in very good agreement with experimental As–As bond lengths in neutral *cyclo*-$(AsPh)_6$ (2.459 Å[56]) or anionic $As_6Br_8^{2-}$ (2.430(3)–2.465(3) Å.[57]). Therefore, and due to our experience with the homologous P–X systems, we exclusively rely on the MP2/TZVPP calculations for the following discussion. All calculated species are shown in Fig. 9 which include important distances and bond angles, partial charges and shared electron numbers for selected atoms and bonds.

$PX_3$, $PX_2^+$, $P_2X_5^+$ and $PX_4^+$ (X = Br, I) used in the thermodynamic calculations were calculated earlier;[24] in this paper neither their geometries nor structural parameters are shown (their total energies, ZPEs, COSMO solvation energies, thermal and entropic contributions are given in the supplemental material). The arsenic cations and molecules have similar geometries to the homologous phosphorus species. Fig. 9 also includes the geometry of $AsI_2PI_3^+$ and $PI_2AsI_3^+$ cations.

**$Ag(CH_2Cl_2)_3^+$.** To get more reliable results for our thermodynamic calculations we replaced the naked $Ag^+$ ion by its tris(methylene chloride) complex (see Fig. 10) that was found in the crystal structure of $(CH_2Cl_2)_3Ag^+[Al(OR)_4]^-$,[58] as well as $(CH_2Cl_2)_3Ag^+[(RO)_3Al–F–Al(OR)_3]^-$.[36] The structure of such a solvated silver cation is also present in $CH_2Cl_2$ solution and, as will be shown, is important for the entropic balance. The starting geometry was taken from the X-ray data and calculated in $C_2$ symmetry.[36,58]

**Anion decomposition by $EX_2^+$ and $E_2X_5^+$.** To estimate the reactivity of the $EX_2^+$ salts in a decomposition reaction (eqn. (15)), we calculated the four products of a $RO^-$ ligand abstraction from the $[Al(OR)_4]^-$ anion (Fig. A, ESI†): $EX_2OR$ ($C_1$) (X = Br, I; E = P, As). Those species were only calculated at

**Table 2** The IR frequencies of the mixture of $I_2As–PI_3^+$ and $P_2I_5^+$ cations. The vibrations of the pure $P_2I_5^+$ salt are also included as well as the MP2/TZVPP calculated frequencies of the $I_2As–PI_3^+$ and $P_2I_5^+$ cations[c]

| Fractions (I)/(II) | $I_2As–PI_3^+$ in (I)/(II) | $P_2I_5^+$ in (I)/(II)[24] | Pure $P_2I_5^+$ | $I_2As–PI_3^+$ MP2/TZVPP Int. (sym.) (IR:%) | $P_2I_5^+$ MP2/TZVPP Int. (sym.) (IR:%) |
|---|---|---|---|---|---|
| 440[a] | 440[a] | 440[a] | 430 (sh) | 443 (a′) (98) | 462 (a′) (59) |
| 412 (s) | — | 412 (s) | 413 (s) | — | 437 (a″) (100) |
| 408 (vs) | 408 (vs) | | — | 433 (a″) (100) | — |
| 402 (s) | — | 402 (s) | 401 (s) | — | 420 (a′) (66) |
| 375 (s) | 375 (s) | — | — | 394 (a′) (34) | — |
| 364 (s) | — | 364 (s) | 364 (s) | — | 389 (a″) (63) |
| 334 (m) | | 334 (m) | 330 (s) | — | 354 (a′) (23) |
| 247 (m) | 247 (m) | — | — | 268 (a″) (38) | — |
| 237 (w) | 237 (w) | — | — | 254 (a′) (11) | — |
| 223 (m) | — | 223 (m) | 223 (m) | — | 235 (a′) (23) |
| 206 (w)[b] | — | — | | — | — |
| | | | | 185 (a′) (14) | 142 (a′) (2) |
| | | | | 127 (a′) (4) | 107 (a″) (0) |
| | | | | 100 (a″) (0) | 105 (a′) (1) |
| | | | | 92 (a′) (2) | 88 (a′) (0) |
| | | | | 84 (a′) (0) | |
| | | | | 69 (a″) (0) | |
| | | | | 63 a′ (0) | |
| | | | | 50 (a′) (0) | |
| | | | | 42 (a″) (0) | |
| | | | | 25 (a″) (0) | |

[a] One vibration of $I_2As–PI_3^+$ (calc. 443 $cm^{-1}$) overlapped with $P_2I_5^+$ and anion vibration (at 445 $cm^{-1}$) and is therefore not seen. [b] $AsI_3$ (*cf.* Raman spectrum of pure $AsI_3$ at 207 $cm^{-1}$). [c] "Fraction (I)" denotes the first fraction of more crystalline product, the "Fraction (II)" fraction was obtained from the filtrate after crystallization by removing the solvent *in vacuo*.

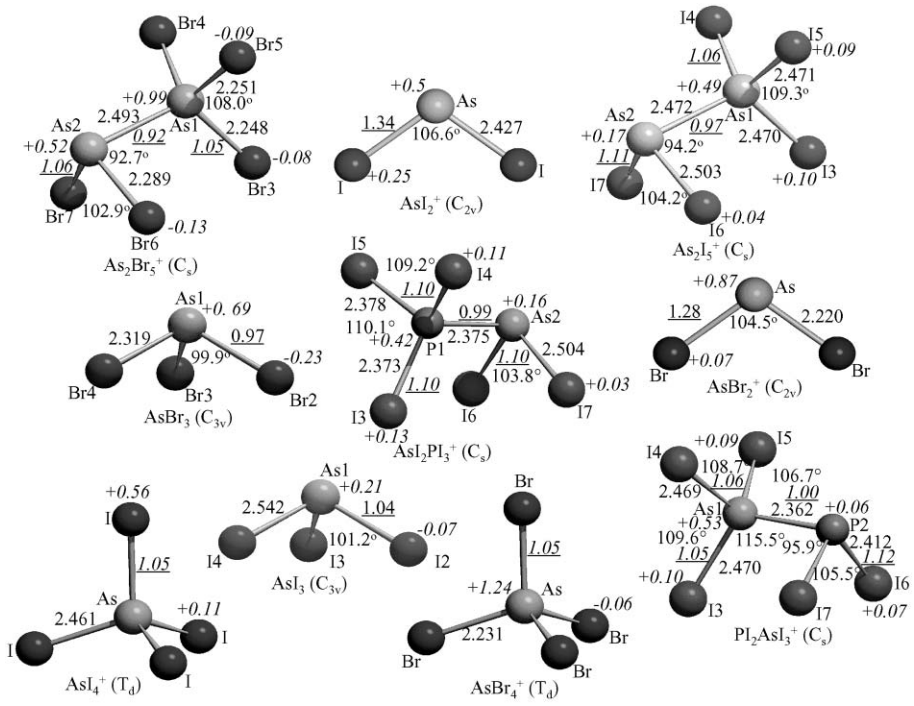


**Fig. 9** The MP2/TZVPP minimum geometries of the arsenic-halogen species $As_2X_5^+$ ($C_s$), $AsX_4^+$ ($T_d$), $AsX_2^+$ ($C_{2v}$), $AsX_3$ ($C_{3v}$), $AsI_2PI_3^+$ ($C_s$) and $PI_2AsI_3^+$ ($C_s$) (X = Br, I). Calculated partial charges ("Paboon") are given in italics, shared electron numbers (SEN) are given in italics and are underlined. All species are true minima with no imaginary frequencies.

the BP86/SVP level, since the geometries of the other reaction participators in eqn. (15), $Al(OR)_3$ and $Al(OR)_4^-$, could only be calculated at this lower level.[40] However, the used reactions are all isodesmic. Therefore, we expect the results to be reliable. The results are included in the Discussion below (Table 3).

## Discussion

According to the information in the Initial calculations section, the formation of $AsX_2^+$ is almost as likely as that of $PX_2^+$. However, the experiments proved that the "$AsBr_2^+$" intermediate is formed only above −30 °C, while "$PX_2^+$" (X = Br, I) intermediates are already formed at −78 °C. Moreover, "$AsBr_2^+$" is much more reactive than "$PX_2^+$" and completely decomposed the anion in all reactions. Neither $P_4AsBr_2^+$ (eqn. (9)) nor $As_2Br_5^+$ (eqn. (8), X = Br) could be obtained. The only As containing product was the $AsBr_4^+$ salt obtained by the reaction of $AsBr_3$, $Br_2$ and $Ag[Al(OR)_4]$. In contrast to the smooth reactions of $PI_3$ with the silver salt leading to the $P_2I_5^+$ salt, no reaction occurred between $AsI_3$ and $Ag[Al(OR)_4]$ and an "$AsI_2^+$" intermediate was never formed. Instead of $AsI_3$, diiodine reacted with the silver cation in the reaction between $AsI_3$, $I_2$ and

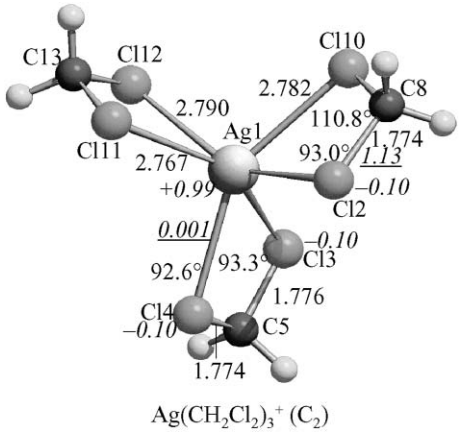


**Fig. 10** The silver tris(methylene chloride) complex $Ag(CH_2Cl_2)_3^+$ ($C_2$). Calculated partial charges ("Paboon") are given in italics, shared electron numbers (SEN) are given in italics and are underlined. This species is a true minimum with no imaginary frequencies.

$Ag[Al(OR)_4]$, forming an unknown but very reactive species that completely decomposed the anion. In the reaction between $AsI_3$, $PI_3$ and the silver salt only the products of the insertion of a "$PI_2^+$" intermediate in the P–I bond of $PI_3$ ($\rightarrow P_2I_5^+$) and As–I bond of $AsI_3$ ($\rightarrow I_2As–PI_3^+$) were obtained. No evidence for the presence of an "$AsI_2^+$" intermediate was observed. In the following we want to shed light on these puzzling facts.

### On the $AsBr_2^+$ intermediate

We showed that the formation of "$AsBr_2^+$" only led to the decomposition of the anion. Why does the decomposition of the anion dominate over the formation of $As_2Br_5^+$ and $P_4AsBr_2^+$?

A possible answer is that the "$AsBr_2^+$" cation is very reactive and is too short lived to insert in the As–Br or P–P bond of $AsBr_3$ or $P_4$.[59] To support this assumption, we compared the reactivity of "$EX_2^+$" in a simple isodesmic ligand abstraction reaction (eqn. (15)) from which the relative (thermodynamic) stability of the $EX_2^+$ cations with the $[Al(OR)_4]^-$ anion may be extracted (E = As, P; X = Br, I; Table 3).[60]

$$EX_2^+[Al(OR)_4]^- \rightarrow EX_2OR + Al(OR)_3 \quad (E = P, As; X = Br, I; R = C(CF_3)_3) \qquad (15)$$

According to the calculated thermodynamic data $AsI_2^+[Al(OR)_4]^-$ would be more stable than $PI_2^+[Al(OR)_4]^-$ and $AsBr_2^+[Al(OR)_4]^-$ should be more stable than $PBr_2^+[Al(OR)_4]^-$. This contrasts with the experiment. The observed reactivity of the "$EX_2^+$" intermediate increases according to: "$PI_2^+$" < "$PBr_2^+$" ≪ "$AsBr_2^+$". The calculations indicate that gaseous $PX_2^+$ is indeed more reactive, however, at low temperature in solution it has to be almost absent, since we have never found direct evidence for the presence of $PX_2^+$.[24] In solution the $PX_2^+$ cations are incorporated in equilibrium (16) (E = P).

In the above equilibrium practically no free $PX_2^+$ is present but only $P_2X_5^+$ at low temperature. It was shown experimentally[24] that even if a 1 : 1 $Ag^+ : PX_3$ stoichiometry was present, only the $P_2X_5^+$ cation is formed in the reaction and the NMR-signal of $PX_2^+$, if not involved in rapid exchange, was below the detection limit at −90 °C. However, supporting the equilibrium in eqn. (16), the $P_2Br_5^+[Al(OR)_4]^-$ salt can be used as a source of "$PBr_2^+$" in an insertion reaction with $P_4$ giving cleanly $P_5Br_2^+$ and $PBr_3$. What is the situation for $AsX_2^+$? Thermodynamic calculations show clearly that in solution the participation of $AsBr_2^+$ in such equilibrium is substantially greater than in the case of all other cations (Table 4).

**Table 4** $\Delta H^\circ_{(g)}$, $\Delta G^\circ_{(g)}$ and $\Delta G^\circ_{(CH_2Cl_2)}$ for equilibrium (16)

| Reaction | $\Delta H^\circ_{(g)}$ | $\Delta G^\circ_{(g)}$ | $\Delta G^\circ_{(CH_2Cl_2)}$ |
|---|---|---|---|
| $As_2Br_5^+ \rightarrow AsBr_3 + AsBr_2^+$ | +144 | +90 | +30 |
| $As_2I_5^+ \rightarrow AsI_3 + AsI_2^+$ | +178 | +124 | +70 |
| $P_2Br_5^+ \rightarrow PBr_3 + PBr_2^+$ | +197 | +138 | +82 |
| $P_2I_5^+ \rightarrow PI_3 + PI_2^+$ | +222 | +161 | +109 |

$$E_2X_5^+ \rightleftharpoons EX_3 + EX_2^+ \quad (E = As, P; X = Br, I) \qquad (16)$$

Equilibrium (16) is only endergonic by +30 kJ mol$^{-1}$ for $As_2Br_5^+$. In contrast, all other cations form considerably less likely (endergonic by +70 to +109 kJ mol$^{-1}$). More specifically, $PBr_2^+$ formation from $P_2Br_5^+$ is by +52 kJ mol$^{-1}$ less favorable than $AsBr_2^+$ from $As_2Br_5^+$. This means that the latter is far more reactive and the equilibrium concentration of $AsBr_2^+$ is so high that it immediately decomposes the anion. Eqn. (16) may further be shifted to the right hand side by complex formation of $EX_2^+$ with $CH_2Cl_2$. It was shown[24] that complexation of $PBr_2^+$ with $CH_2Cl_2$ giving $[PBr_2 \cdots ClCH_2Cl]^+$ is favorable by about 50 kJ mol$^{-1}$. In summary it is therefore likely to assume that by additional $CH_2Cl_2$ coordination, the $As_2Br_5^+$ equilibrium (16) may completely be shifted to the right hand side. This is in good agreement with our experiments. The reaction of $AsBr_3$ and $Ag[Al(OR)_4]$ did not occur below −30 °C, probably due to kinetic reasons, and above this temperature the intermediately formed $AsBr_2^+$ completely decomposed the anion.

From the preceding it is clear that $E_2X_5^+$ (in equilibrium with $EX_2^+$ and $EX_3$) is the true reactive cation in solution. To understand the experimental reactivity trends, one has to assess the anion stability in the presence of the $E_2X_5^+$ cation. Therefore, we combined the ligand abstraction reactions in eqn. (15) (BP86/SVP level) with the $E_2X_5^+$ equilibrium (16) (MP2/TZVPP level) to obtain the thermodynamics of decomposition of the anion by the $E_2X_5^+$ cations (by addition of the enthalpies of both reactions). The values of $\Delta H_{(g)}$, $\Delta G^\circ_{(g)}$ and $\Delta G^\circ_{(CH_2Cl_2)}$ for this decomposition are collected in Table 5.

The $\Delta G^\circ_{(CH_2Cl_2)}$ values in Table 5 are in very good agreement with the experiments. The decomposition of the $P_2Br_5^+[Al(OR)_4]^-$ salt occurs at 0 °C and proceeds quickly at room temperature (few hours), the $P_2I_5^+$ salt can be handled with less care at 0 °C and the $As_2Br_5^+$ salt (better described as $AsBr_2^+$) does not survive even at −30 °C!

According to Table 5 and in comparison to known $P_2Br_5^+$, the relative stability of the $As_2I_5^+$ cation looks promising. Therefore, $As_2I_5^+$ would be a good candidate to be prepared by a suitable (new) route.

**Table 3** $\Delta H^\circ_{(g)}$, $\Delta G^\circ_{(g)}$, $\Delta G^\circ_{(CH_2Cl_2)}$ of the isodesmic decomposition according to eqn. (15) calculated at the BP86/SVP level

| Decomposition of $EX_2^+[Al(OR)_4]^-$ | $\Delta H^\circ_{(g)}$[a] | $\Delta G^\circ_{(g)}$[a] | $\Delta G^\circ_{(CH_2Cl_2)}$ |
|---|---|---|---|
| $AsBr_2^+ + Al(OR)_4^- \rightarrow AsBr_2OR + Al(OR)_3$ | −397 | −393 | −88 |
| $AsI_2^+ + Al(OR)_4^- \rightarrow AsI_2OR + Al(OR)_3$ | −357 | −354 | −68 |
| $PBr_2^+ + Al(OR)_4^- \rightarrow PBr_2OR + Al(OR)_3$ | −426 | −418 | −111 |
| $PI_2^+ + Al(OR)_4^- \rightarrow PI_2OR + Al(OR)_3$ | −387 | −380 | −91 |

[a] The enthalpies in the gas phase are high since two charged species react to give two neutrals.

**Table 5** $\Delta H^\circ_{(g)}$, $\Delta G^\circ_{(g)}$ and $\Delta G^\circ_{(CH_2Cl_2)}$ for the decomposition of $E_2X_5^+[Al(OR)_4]^-$

| Reaction of the decomposition of $E_2X_5^+[Al(OR)]_4^-$ | $\Delta H^\circ_{(g)}$ | $\Delta G^\circ_{(g)}$ | $\Delta G^\circ_{(CH_2Cl_2)}$ |
|---|---|---|---|
| $As_2Br_5^+ + Al(OR)_4^- \rightarrow AsBr_2OR + AsBr_3 + Al(OR)_3$ | −254 | −303 | −59 |
| $As_2I_5^+ + Al(OR)_4^- \rightarrow AsI_2OR + AsI_3 + Al(OR)_3$ | −179 | −230 | +3 |
| $P_2Br_5^+ + Al(OR)_4^- \rightarrow PBr_2OR + PBr_3 + Al(OR)_3$ | −230 | −281 | −29 |
| $P_2I_5^+ + Al(OR)_4^- \rightarrow PI_2OR + PI_3 + Al(OR)_3$ | −166 | −219 | +19 |

### The formation of $AsI_2$–$PI_3^+$

The reaction between $PI_3$, $AsI_3$ and $Ag[Al(OR)_4]$ proceeds according to a similar mechanism to that for the $E_2X_5^+$ cations. $I_2As$–$PI_3^+$ would be the product of a "$PI_2^+$" insertion in the As–I bond and $I_2P$–$AsI_3^+$ the product of an "$AsI_2^+$" insertion into the P–I bond. The latter is by +27 kJ mol$^{-1}$ less favorable than the first (MP2/TZVPP), which is in agreement with the experiment ($I_2As$–$PI_3^+$ formation). Therefore, $AsI_2$–$PI_3^+$ is the kinetically and thermodynamically favored product. However, $P_2I_5^+$ was also formed in the reaction mixture. Thus $AsI_3$ and $PI_3$ compete in the insertion reaction with "$PI_2^+$" (see eqn. (17)).

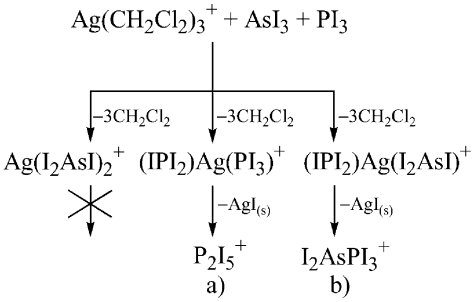


(17)

$\Delta G^\circ_{(CH_2Cl_2)}$ for reaction (17a) is −203 kJ mol$^{-1}$ and for (17b) −199 kJ mol$^{-1}$ (including $AgI_{(s)}$). The almost equal thermodynamics of the reactions explains the 1 : 1 ratio of the products of the reaction. Interestingly, excess $AsI_3$ added to the reaction mixture did not change the product ratio. In agreement with this, the reaction of $P_2I_5^+$ with $AsI_3$ (eqn. (18)) is endergonic by +4 kJ mol$^{-1}$ (MP2/TZVPP).

$$P_2I_5^+ + AsI_3 \rightarrow I_2AsPI_3^+ + PI_3;\ \Delta G^\circ_{(CH_2Cl_2)} = +4\ \text{kJ mol}^{-1} \quad (18)$$

Additionally, the poor solubility of $AsI_3$ at low temperature influences eqn. (18): The equilibrium concentration of $PI_3$ is higher than that of $AsI_3$ and the maximum concentration of $AsI_3$ thus limits the amount of $I_2As$–$PI_3^+$ formed.

## Conclusions

### Preparation of $AsBr_4^+$ and $I_2As$–$PI_3^+$

$AsBr_4^+$ is the only As–X cation that could be prepared using the "$AsX_2^+$" insertion route. $AsBr_4^+[Al(OR)_4]^-$ is the second structurally characterized representative of a $AsBr_4^+$ cation. It was also characterized by IR and $^{75}$As NMR spectroscopy. The successfully prepared $I_2As$–$PI_3^+[Al(OR)_4]^-$ salt is, to the best of our knowledge, the first mixed As/P-halogen cation. It is the product of a "$PI_2^+$" insertion into the As–I bond of the $AsI_3$ molecule. Its structure could be assigned based on $^{31}$P NMR and IR spectroscopy (as a mixture with $P_2I_5^+$) as well as quantum-chemical calculations.

### The failure to prepare $AsI_4^+$

In contrast to all other investigated $Ag^+/X_2/EX_3$ mixtures, $AsI_4^+[Al(OR)_4]$ salts can not be prepared by this route, although its formation would thermodynamically be possible. Instead it is likely that a $Ag(I_2)_x^+$ cation forms as an intermediate which reacts above 0 °C by separation of solid AgI giving products that completely decompose the anion.

### The failure to prepare $As_2X_5^+$

It was shown earlier that $P_2X_5^+$ is in equilibrium with the "$PX_2^+$" cation, likely as its $CH_2Cl_2$ solvate. For X = Br this equilibrium may be used as an experimental source of "$PBr_2^+$".[24] According to the current investigations, the same equilibrium takes places for $As_2Br_5^+$, but lies in this case almost completely on the (solvated) "$AsBr_2^+$" side. This carbenoid cation is to reactive to be handled in the presence of the $[Al(OR)_4]^-$ anion even at very low temperature. Therefore, all attempts to prepare $As_2Br_5^+[Al(OR)_4]^-$, $AsBr_2^+[Al(OR)_4]^-$ as well as $P_4AsBr_2^+[Al(OR)_4]^-$ salts failed and instead led to anion decomposition. The $As_2I_5^+$ cation appears to be a likely candidate for a successful synthesis with a stability that would be expected to lie between the known $P_2Br_5^+$ and $P_2I_5^+$. However, the only in low concentration formed $Ag(AsI_3)_2^+$ complex is kinetically stable against heterolytic As–I bond cleavage and no evidence for the formation of $As_2I_5^+$ could be presented.

## Experimental

All manipulations were performed using standard Schlenk or dry box techniques and a dinitrogen or argon atmosphere ($H_2O$ and $O_2$ < 1 ppm). Apparatus were closed by J. Young valves. All solvents were rigorously dried over $P_2O_5$ and degassed prior to use and stored under $N_2$. $AsBr_3$ was prepared from arsenic trioxide, sulfur and bromine according to the method described in the literature[61] and $AsI_3$ was prepared from $As_2O_3$, KI and HCl according to the literature.[62,63] $PI_3$ was prepared by reacting white phosphorus and iodine in $CS_2$. $PBr_3$ (Fluka), $I_2$ and $Br_2$ (Merck) were purified prior to use by distillation, sublimation or recrystallization. Purity of those halides was checked by Raman spectroscopy. The silver aluminate $Ag[Al(OR)_4]$ was prepared according to the literature.[39] Raman and IR spectra were recorded using a 1064 nm laser on a Bruker IFS 66v spectrometer equipped with the Raman modul FRA 106. IR spectra were recorded in Nujol mull between CsI plates. NMR spectra (Bruker AC250) of sealed samples were run in $CD_2Cl_2$ and were referenced towards the solvent ($^1$H, $^{13}$C) and external aqueous $AlCl_3$ ($^{27}$Al), 85% $H_3PO_4$ ($^{31}$P), $CF_3COOH$ ($^{19}$F) or $NaAsF_6$ in $d_3$-acetonitrile.

### Reactions between $AsI_3$, $PI_3$ and $Ag[Al(OR)_4]$

**Reaction (1) (in $CH_2Cl_2$).** $Ag[Al(OR)_4]$ (0.953 g, 0.887 mmol) and $AsI_3$ (0.410 g, 0.887 mmol) and were loaded into a two-bulb vessel with an internal dropping funnel (two pieces connected by a flange with viton O-ring and Teflon inlay). $PI_3$ (0.368 g, 0.887 mmol) was placed in the dropping funnel and dissolved in $CH_2Cl_2$ (30 ml). A few ml of $CH_2Cl_2$ were placed in stirred mixture of $AsI_3$/$Ag[Al(OR)_4]$. The flask was cooled to about −78 °C and the dissolved $PI_3$ was added slowly in the course of 60 min. After addition of the entire $PI_3$, the reaction mixture was stirred for 3 days at temperatures below −30 °C. A $^{31}$P NMR spectrum of about 3 ml of the clear orange solution was prepared by removing all volatiles *in vacuo* and addition $CD_2Cl_2$ (1 ml) (sample 1). An additional equivalent of $AsI_3$ (0.402 g, 0.884 mmol) was added to the mixture *via* the funnel supported by $CS_2$ (5 ml). After 2 days stirring at −30 °C from 2 ml of the solution another NMR sample was prepared as before (sample 2).

Sample 1: $^{13}$C NMR (63 MHz, $CD_2Cl_2$, −30 °C): $\delta$ 121.0 (q, $J_{CF}$ = 292.5 Hz, $CF_3$ of the $[Al(OR)_4]^-$ anion); $^{27}$Al NMR (78 MHz, $CD_2Cl_2$, −20 °C): $\delta$ 37.1 (s, $\nu_{1/2}$ = 25 Hz); $^{31}$P NMR (101 MHz, $CD_2Cl_2$, −30 °C): $\delta$ 129.7 (d, $J_{PP}$ = 325.1 Hz, $P_2I_5^+$), −157.3 (d, $J_{PP}$ = 325.1 Hz, $P_2I_5^+$), −183.7 (s, $\nu_{1/2}$ = 40 Hz, $AsI_2$–$PI_3^+$). Sample 2: $^{13}$C NMR (63 MHz, $CD_2Cl_2$, −30 °C): $\delta$ 121.0 (q, $J_{CF}$ = 292.4 Hz, $CF_3$ of the $[Al(OR)_4]^-$ anion); $^{27}$Al NMR (78 MHz, $CD_2Cl_2$, −30 °C): $\delta$ 37.4 (s, $\nu_{1/2}$ = 15 Hz); $^{31}$P NMR (101 MHz, $CD_2Cl_2$, −30 °C): $\delta$ 129.7 (d, $J_{PP}$ = 325.3 Hz, $P_2I_5^+$), −157.3 (d, $J_{PP}$ = 325.3 Hz, $P_2I_5^+$), −183.6 (s, $\nu_{1/2}$ = 40 Hz, $AsI_2$–$PI_3^+$); $^{31}$P NMR (101 MHz, $CD_2Cl_2$, −50 °C): $\delta$ 128.0 (d, $J_{PP}$ = 323.4 Hz, $P_2I_5^+$), −156.9 (d, $J_{PP}$ = 323.4 Hz, $P_2I_5^+$), −182.8 (s, $\nu_{1/2}$ = 40 Hz, $AsI_2$–$PI_3^+$).

**Reaction (2) (with 6 equiv. of $AsI_3$ in $CH_2Cl_2$–$CS_2$).** $Ag[Al(OR)_4]$ (0.902 g, 0.773 mmol) was loaded in one bulb of the two bulbed vessel followed by $CH_2Cl_2$ (5 ml). $AsI_3$ (1.758 g, 3.865 mmol) and $PI_3$ (0.320 g, 0.773 mmol) were loaded into the other bulb followed by $CH_2Cl_2$–$CS_2$ mixture in 3 : 1 ratio (15 ml). However, even at room temperature the $AsI_3$ remained mostly undissolved. Both bulbs of the vessel were cooled at −78 °C and solution of the silver salt was poured through the frit plate onto the red suspension of $AsI_3$ and $PI_3$. Precipitation of AgI started below −30 °C and the solution became more orange in color. The reaction was stirred at about −30 °C for 6 h and stored for 4 days in the refrigerator at −30 °C. After this, the solvent was completely removed *in vacuo*. About 5 ml $CH_2Cl_2$ was added to the reaction mixture. The resulting solution was cooled to about −20 °C and filtered at this temperature to get rid off the excess $AsI_3$. The solution was concentrated to about a half and stored at −80 °C. At this temperature after 2 days microcrystalline orange–reddish solids precipitated (fraction I, together with characteristic red crystals of $AsI_3$). The residual solution was evaporated in such a way that the at −80 °C precipitated solids were not contaminated, giving a yellow–orange residue (fraction II). The IR and NMR spectra of both fractions were recorded. The separation of the $I_2As$–$PI_3^+$ from $P_2I_5^+$ salt was unsuccessful and both fractions contain both products but in a different ratio. It should be noted that due to the use of $CS_2$ (lowering of the polarity of the solution) a partial anion decomposition occurred (see $^{13}$C NMR).

Fraction I: $^{13}$C NMR (63 MHz, $CD_2Cl_2$, −30 °C): $\delta$ 120.4 (q, $J_{CF}$ = 290.9 Hz, $CF_3$ of decomposed anion), 120.9 (q, $J_{CF}$ = 291.7 Hz, $CF_3$ of $[Al(OR)_4]^-$); $^{31}$P NMR (101 MHz, $CD_2Cl_2$, −30 °C): $\delta$ 129.5 (d, $J_{PP}$ = 324.5 Hz, $P_2I_5^+$), −157.0 (d, $J_{PP}$ = 324.6 Hz, $P_2I_5^+$), −183.3 (s, $\nu_{1/2}$ = 77 Hz, $AsI_2$–$PI_3^+$). Fraction II: $^{13}$C NMR (63 MHz, $CD_2Cl_2$, −30 °C): $\delta$ 120.4 (q, $J_{CF}$ = 290.7 Hz, $CF_3$ of decomposed anion), 120.9 (q, $J_{CF}$ = 291.9 Hz, $CF_3$ of not decomposed anion); $^{31}$P NMR (101 MHz, $CD_2Cl_2$, −30 °C): $\delta$ 129.5 (d, $J_{PP}$ = 324.4 Hz, $P_2I_5^+$), −157.0 (d, $J_{PP}$ = 324.5 Hz, $P_2I_5^+$), −183.3 (s, $\nu_{1/2}$ = 80 Hz, $AsI_2$–$PI_3^+$). IR: 223 (m, $P_2I_5^+$), 237 (w, $I_2As$–$PI_3^+$), 247 (m, $I_2As$–$PI_3^+$), 290 (m, $[Al(OR)_4]^-$), 315 (m, $[Al(OR)_4]^-$), 334 (m, $P_2I_5^+$), 364 (s, $P_2I_5^+$), 375 (s, $I_2As$–$PI_3^+$), 402 (s, $P_2I_5^+$), 408 (vs, $I_2As$–$PI_3^+$), 412 (s, $P_2I_5^+$), 440 (m, overlapping bands of $I_2As$–$PI_3^+$, $P_2I_5^+$ and $[Al(OR)_4]^-$ vibration at 446 cm$^{-1}$), 446 (s, $[Al(OR)_4]^-$), 537 (s, $[Al(OR)_4]^-$), 560 (m, $[Al(OR)_4]^-$), 579 (m, $[Al(OR)_4]^-$), 636 (m, $[(RO)_3Al$–$F$–$Al(OR)_3]^-$), 728 (s, $[Al(OR)_4]^-$), 755 (w, $[Al(OR)_4]^-$), 831 (m, $[Al(OR)_4]^-$), 864 (m, $[(RO)_3Al$–$F$–$Al(OR)_3]^-$), 975 (vs, $[Al(OR)_4]^-$), 1136 (s, $[Al(OR)_4]^-$), 1161 (s, $[Al(OR)_4]^-$), 1216 (vs, $[Al(OR)_4]^-$), 1248 (vs, $[Al(OR)_4]^-$), 1258 (vs, $[Al(OR)_4]^-$), 1275 (vs, $[Al(OR)_4]^-$), 1305 (s, $[Al(OR)_4]^-$), 1350 (s, $[Al(OR)_4]^-$).

### Synthesis of $AsBr_4^+[Al(OR)_4]^-$:

**Typical large-scale synthesis.** $Ag[Al(OC(CF_3)_3)_4]$ (0.368 g, 0.317 mmol) was weighed into a two bulbed vessel. $AsBr_3$ (0.100 g, 0.317 mmol) and $Br_2$ (0.051 g, 0.317 mmol) followed by $CH_2Cl_2$ (10 ml) were added at −78 °C. The flask was kept at −78 °C and was occasionally shaken until the precipitation of AgBr started. The flask was stored in a −80 °C freezer for 3 days to finish the reaction. The pale yellow-brownish solution was filtered from the solid AgBr, concentrated to about a half and crystallized. $AsBr_4^+[Al(OR)_4]^-$ (R = $C(CF_3)_3$) (0.233 g, 54% yield) was obtained from $CH_2Cl_2$ as slightly yellow block-shaped crystals, sensitive to air and moisture. The crystals are stable under inert atmosphere at r.t. for at least 2 months. The solution is stable for a few hours at 0 °C.

IR (CsI, Nujol mull): $\nu$ 354 (m, $T_2$ $AsBr_4^+$); anion: 281 (w), 315 (w), 330 (vw), 367 (w), 380 (w), 445 (m), 536 (mw), 561 (mw), 572 (w), 727 (s), 756 (w), 833 (m), 973 (vs), 1074 (w, sh), 1131 (m, sh), 1164 (ms), 1222 (vs), 1244 (vs), 1274 (vs), 1298 (s), 1352 (ms) cm$^{-1}$.

**Preparation in the NMR tube.** $Ag[Al(OC(CF_3)_3)_4]$ (0.503 g, 0.434 mmol) and $AsBr_3$ (0.137 g, 0.434 mmol) were transferred into a NMR tube glass-blown onto a J. Young valve followed by condensing 1 ml of $CD_2Cl_2$ onto the mixture at −78 °C. At this temperature $Br_2$ (0.069 g, 0.022 ml, 0.434 mmol) was added to the mixture with a calibrated 100 µl syringe. The NMR tube was flame-sealed under vacuum and stored overnight at −78 °C. Before the spectra were recorded, the tube was warmed to −20 °C, shaken a few times until the precipitation of AgBr appeared to be complete.

$^{13}$C NMR (63 MHz, $CD_2Cl_2$, −30 °C): $\delta$ 120.9 (q, $J_{CF}$ = 292.7 Hz, $CF_3$); $^{27}$Al NMR (78 MHz, $CD_2Cl_2$, +25 °C): $\delta$ 36.0 (s, $\nu_{1/2}$ = 15 Hz); $^{75}$As NMR (51 MHz, $CD_2Cl_2$, −70 °C): $\delta$ −148.2 (s, $\nu_{1/2}$ = 983.2 Hz).

**Formation of $[(RO)_2AlF(THF)]_2$.** $Ag[Al(OR)_4]$ (1.077 g, 0.862 mmol) and $AsBr_3$ (0.588 g, 1.724 mmol) were transferred into a two bulbed vessel under argon atmosphere. The mixture was kept at room temperature. The reaction started immediately after mixing the starting materials (occasionally shaken) resulting in a softening of the mixture simultaneously with changing of the color. The slightly brown mixture became liquid for a short time and than solidified again with precipitation of AgBr. The mixture was extracted three times with pentane and concentrated. Thereby crystals of $AsBr_3$ formed. After removal of all volatiles from the extract a white residue remained, that got dark within a few minutes. After removing all volatiles the residue weighted 0.836 g (loss of weight 49%). The residue was dissolved in 3 : 1 $CH_2Cl_2$–THF and stored at −30 °C. Colorless crystals of $[(RO)_2AlF(THF)]_2$ were grown from this solution and isolated (0.473 g, 88% yield based on Al in $Ag[Al(OR)_4]$).

$^1$H NMR (250 MHz, $CD_2Cl_2$, +25 °C): $\delta$ 4.28 (m, O–$CH_2$, THF), 2.13 (m, $CH_2$, THF); $^{13}$C NMR (63 MHz, $CD_2Cl_2$, +25 °C): $\delta$ 121.1 (q, $J_{CF}$ = 290.8 Hz, $CF_3$), 74.5 (s, –$OCH_2$–, THF), 73.7 (s, $OCH_2$, THF), 25.5 (s, $CH_2$, THF), 25.3 (s, $CH_2$, THF).

### X-Ray crystal structure determinations

Data collection for X-ray structure determinations (Table 6) were performed on a STOE IPDS II diffractometer using graphite-monochromated Mo–Kα (0.71073 Å) radiation. Single crystals were mounted in perfluoroether oil on top of a glass fiber and then brought into the cold stream of a low-temperature device so that the oil solidified. All calculations were performed on PC's using the SHELX97 software package. The structures were solved by direct methods and successive interpretation of the difference Fourier maps, followed by least-squares refinement. The crystals of **1** were racemically twinned. Solving structure in the *Pna*2$_1$ space group and applying the appropriate twin law gave in the final refinement $R_1$ = 0.0394 ($wR2$ = 0.0861) see table below. Six (–$CF_3$) groups of the anion in **1** had to be split over two positions and the disordered atoms were included in the refinement giving an occupation number of 30% for the disordered atoms. The positions of all $CF_3$ groups were fixed with SADI restraints. The hydrogen atoms of the coordinated THF molecule in $[(RO)_2AlF(THF)]_2$ were found in

**Table 6** X-Ray structure data for $AsBr_4^+[Al(OR)_4]^-$ and $[(RO)_2AlF(THF)]_2$

| | $AsBr_4^+[Al(OR)_4]^-$ | $[(RO)_2AlF(THF)]_2$ |
|---|---|---|
| Crystal size/mm | 0.3 × 0.1 × 0.1 | 0.2 × 0.6 × 0.8 |
| Crystal system | Orthorhombic | Monoclinic |
| Space group | $Pna2_1$ | $P2_1/n$ |
| $a$/Å | 19.062(4) | 9.652(2) |
| $b$/Å | 13.874(3) | 12.727(3) |
| $c$/Å | 13.588(3) | 15.596(3) |
| $\alpha$/° | 90 | 90 |
| $\beta$/° | 90 | 96.34(3) |
| $\gamma$/° | 90 | 90 |
| $V$/Å$^3$ | 3593.6(1) | 1904.1(7) |
| $Z$ | 4 | 2 |
| $D_c$/Mg m$^{-3}$ | 2.517 | 2.052 |
| $\mu$/mm$^{-1}$ | 5.634 | 0.304 |
| Max., min. trans. | 0.3910, 0.5391 | — |
| Index ranges, $hkl$ | −21 to 21, −17 to 16, −16 to 16 | −9 to 11, −13 to 15, −18 to 19 |
| $2\theta$/° | 51.9 | 51.7 |
| $T$/K | 200(2) | 100(2) |
| Refl. collected | 22082 | 7799 |
| Refl. unique | 6572 | 3426 |
| Refl. observed ($2\sigma$) | 3485 | 2749 |
| $R_{int}$ | 0.0707 | 0.0411 |
| GOOF/GOOF restrained | 0.855/0.852 | 1.009/1.009 |
| Final $R/wR2$ ($2\sigma$) | 0.0394/0.0861 | 0.0301/0.0710 |
| Final $R/wR2$ (all data) | 0.0925/0.1022 | 0.0435/0.0750 |
| Larg. res. peak/e Å$^{-3}$ | 0.529 | 0.266 |

the difference Fourier map and included isotropically into the refinement. All other atoms were refined anisotropically.

CCDC reference numbers 256551 and 256552.

See http://www.rsc.org/suppdata/dt/b4/b417629d/ for crystallographic data in CIF or other electronic format.

### Computational details

All computations were done with the program TURBOMOLE.[64,65] The geometries of all species were optimized at the (RI-)MP2 level[46] with the triple ζ valence polarization (two d and one f functions) TZVPP basis set.[44,45] The 28 and 46 electron cores of Ag and I were replaced by a quasi relativistic effective core potential.[47] All species were also fully optimized at the BP86/SV(P) (DFT-)level[66–70] albeit these geometries are not shown. Approximate solvation energies ($CH_2Cl_2$ solution with $\varepsilon_r = 8.93$) were calculated with the COSMO model[71] at the BP86/SV(P) (DFT-)level using the MP2/TZVPP geometries. Frequency calculations were performed for all species and structures represent true minima without imaginary frequencies on the respective hypersurface. For thermodynamic calculations the zero point energy and thermal contributions to the enthalpy and the free energy at 298 K have been included.[72] The calculation of the thermal contributions to the enthalpy and entropic contributions to the free energy were done with TURBOMOLE. For all species a modified Roby–Davidson population analysis based on occupation numbers (Paboon) has been performed using the (RI-)MP2/TZVPP electron density.

## References


1 J. Petersen, E. Lork and R. Mews, *Chem. Commun.*, 1996, 1897–1898.
2 M. Binnewies, M. Jäckel and H. Willner, *Anorganische und Allgemeine Chemie,* Spektrum Akademischer Verlag, Heidelberg and Berlin, 1st edn., 2004.
3 I. R. Beattie and K. M. S. Livingston, *J. Chem. Soc. A*, 1969, **5**, 859–860.
4 F. J. J. Brinkmann, H. Gerding and K. Olie, *Recl. Trav. Chim. Pays-Bas*, 1969, **88**, 1358–1360.
5 S. Haupt and K. Seppelt, *Z. Anorg. Allg. Chem.*, 2002, **628**, 729–734.
6 K. Seppelt, *Z. Anorg. Allg. Chem.*, 1977, **434**, 5–15.
7 K. Seppelt, *Angew. Chem.*, 1976, **88**, 410–411.
8 F. Claus, M. Glaser and R. Minkwitz, *Z. Anorg. Allg. Chem.*, 1983, **506**, 178–184.
9 F. Claus, M. Glaser, V. Woelfel and R. Minkwitz, *Z. Anorg. Allg. Chem.*, 1984, **517**, 207–214.
10 V. F. Claus and R. Minkwitz, *Z. Anorg. Allg. Chem.*, 1983, **501**, 19–26.
11 R. Minkwitz and H. Prenzel, *Z. Anorg. Allg. Chem.*, 1986, **534**, 150–152.
12 R. Minkwitz, H. Prenzel, A. Schardey and H. Oberhammer, *Inorg. Chem.*, 1987, **26**, 2730–2732.
13 A. F. Holleman, E. Wiberg and N. Wiberg,*Lehrbuch der Anorganischen Chemie*, Walter de Gruyter, Berlin and New York, 101st edn., 1995.
14 $PI_5$ is present in many text books as "compound in bottle", however, we found that its characterization is limited only to the melting point! According to our unpublished experimental results, $PI_5$ could not be obtained by the route by which it was claimed to be synthesized (starting from $POCl_3$ and LiI, see ref. 13). This will be the subject of a paper, currently in preparation.
15 B. W. Tattershall and N. L. Kendall, *Polyhedron*, 1994, **13**, 1517–1521.
16 M. Baudler, D. Grenz, U. Arndt, H. Budzikiewicz and M. Feher, *Chem. Ber.*, 1988, **121**, 1707–1709.
17 K. B. Dillon and B. Y. Xue, *Inorg. Chim. Acta*, 2001, **320**, 172–173.
18 C. Aubauer, M. Kaupp, T. M. Klapötke, H. Nöth, H. Piotrowski, W. Schnick, J. Senker and M. Suter, *J. Chem. Soc., Dalton Trans.*, 2001, 1880–1889.
19 C. Aubauer, M. Klapötke and A. Schulz, *Int. J. Vib. Spec.*, 1999, **3**.
20 C. Aubauer and T. M. Klapötke, *Int. J. Vib. Spec.*, 2001, **5**.
21 M. Kaupp, C. Aubauer, G. Engelhardt, T. M. Klapötke and O. L. Malkina, *J. Chem. Phys.*, 1999, **110**, 3897–3902.
22 S. Pohl, *Z. Anorg. Allg. Chem.*, 1983, **498**, 15–19.
23 I. Tornieporth-Oetting and T. Klapötke, *J. Chem. Soc., Chem. Commun.*, 1990, 132–133.
24 M. Gonsior, I. Krossing, L. Müller, I. Raabe, M. Jansen and L. Van Wullen, *Chem. Eur. J.*, 2002, **8**, 4475–4492.
25 I. Krossing and I. Raabe, *Angew. Chem., Int. Ed.*, 2001, **40**, 4406–4409.
26 G. S. H. Chen and J. Passmore, *J. Chem. Soc., Dalton Trans.*, 1979, 1251–1256.
27 G. S. H. Chen and J. Passmore, *J. Chem. Soc., Chem. Commun.*, 1973, 559.
28 R. Minkwitz, J. Nowicki and H. Borrmann, *Z. Anorg. Allg. Chem.*, 1991, **596**, 93–98.
29 M. Gerken, P. Kolb, A. Wegner, H. P. A. Mercier, H. Borrmann, D. A. Dixon and G. J. Schrobilgen, *Inorg. Chem.*, 2000, **39**, 2813–2824.
30 I. Tornieporth-Oetting and T. Klapötke, *Angew. Chem.*, 1989, **101**, 1742–1744.
31 M. Broschag, T. M. Klapötke and I. C. Tornieporth-Oetting, *J. Chem. Soc., Chem. Commun.*, 1992, 446–448.
32 R. E. Pabst, M. C. Sharpe, J. L. Margrave and J. L. Franklin, *Int. J. Mass Spectrom. Ion Phys.*, 1980, **33**, 187–199.

33 H. L. Sievers, H.-F. Grützmacher, H. Grützmacher and S. Pitter, *J. Am. Chem. Soc.*, 1995, **117**, 2313–2320.
34 C. Aubauer, G. Engelhardt, T. M. Klapötke and A. Schulz, *J. Chem. Soc., Dalton Trans.*, 1999, 1729–1734.
35 I. Krossing, *J. Chem. Soc., Dalton Trans.*, 2002, 500–512.
36 A. Bihlmeier, M. Gonsior, I. Raabe, N. Trapp and I. Krossing, *Chem. Eur. J.*, 2004, **10**, 5041–5051.
37 I. Krossing, H. Brands, R. Feuerhake and S. Koenig, *J. Fluorine Chem.*, 2001, **112**, 83–90.
38 I. Krossing, *J. Am. Chem. Soc.*, 2001, **123**, 4603–4604.
39 I. Krossing, *Chem. Eur. J.*, 2001, **7**, 490–502.
40 I. Krossing and I. Raabe, *Angew. Chem., Int. Ed.*, 2004, **43**, 2066–2090.
41 M. Gonsior, I. Krossing and E. Matem, *Eur. J. Chem.*, submitted.
42 H. D. B. Jenkins, I. Krossing, J. Passmore and I. Raabe, *J. Fluorine Chem.*, 2004, **125**, 1585–1592.
43 I. Krossing and I. Raabe, *Chem. Eur. J.*, 2004, **10**, 5017–5030.
44 A. Schäfer, H. Horn and R. Ahlrichs, *J. Chem. Phys.*, 1992, **97**, 2571.
45 A. Schäfer, C. Huber and R. Ahlrichs, *J. Chem. Phys.*, 1994, **100**, 5829.
46 F. Weigend and M. Häser, *Theor. Chim. Acta*, 1997, **97**, 331.
47 W. Kuechle, M. Dolg, H. Stoll and H. Preuss, *Mol. Phys.*, 1991, **74**, 1245.
48 The sublimation energies for the formation of solid silver halide were included. The sublimation energy for the process $AgI_{(g)} \rightarrow AgI_{(s)} = -196.9$ kJ mol$^{-1}$ and for $AgBr_{(g)} \rightarrow AgBr_{(s)} = -217.4$ kJ mol$^{-1}$.
49 T. S. Cameron, J. Passmore and X. Wang, *Angew. Chem., Int. Ed.*, 2004, **43**, 1995–1998.
50 The $[Al(OR)_4]^-$ anion has the usual geometry with Al–O bond lengths at 1.687(2) Å on average and Al–O–C angles that range from 153.7(1) to 162.9(1)°. Therefore, the structure of the anion is affected by librational motion, but correcting all bond distances for librations by a riding model gives the normal $[Al(OR)_4]^-$ values of 1.731–1.740 Å (in $[Ag(C_2H_4Cl_2)_3]^+[Al(OR)_4]^-$ the non corrected Al–O bond lengths are 1.714(3)–1.736(3) Å).
51 M. Gonsior, I. Krossing and N. Mitzel, *Z. Anorg. Allg. Chem.*, 2002, **628**, 1821–1830.
52 C. Cui, H. W. Roesky, M. Noltemeyer, M. F. Lappert, G. Schmidt and H. Hao, *Organometallics*, 1999, **18**, 2256–2261.
53 C. Rennekamp, H. Wessel, H.W. Roesky, P. Müller, H.-G. Schmidt, M. Noltemeyer, I. Usón and A. R. Barron, *Inorg. Chem.*, 1999, **38**, 5235–5240.
54 T. Klapötke and J. Passmore, *J. Chem. Soc., Dalton Trans.*, 1990, 3815–3822.
55 T. Klapötke, J. Passmore and E. G. Awere, *J. Chem. Soc., Chem. Commun.*, 1988, 1426–1427.
56 A. L. Rheingold and P. J. Sullivan, *Organometallics*, 1983, **2**, 327–331.
57 U. Müller and H. Sinnig, *Angew. Chem.*, 1989, **101**, 187–188.
58 I. Krossing and A. Reisinger, unpublished results.
59 For the reaction between $AsBr_3$, $P_4$ and $Ag[Al(OR)_4]$ in solution a complex $[(P_4)Ag(Br_2AsBr)]^+$ should be formed as a intermediate leading to $[P_4AsBr_2]^+$. This complex, however could undergo a dismutation reaction into $[Ag(P_4)_2]^+$ and $[Ag(Br_2AsBr)_2]^+$ according to the equation: $2[(P_4)Ag(Br_2AsBr)]^+ \rightarrow [Ag(P_4)_2]^+ + [Ag(Br_2AsBr)_2]^+$. $\Delta G°(CH_2Cl_2) = +9$ kJ mol$^{-1}$ of this reaction suggests that all the species are present in the solution. Since the reaction of $AsBr_3$ with silver salt (formation of $[Ag(Br_2AsBr)_2]^+$) decomposes the anion at −30 °C, it seems to be very reasonable that the $[(P_4)Ag(Br_2AsBr)]^+$ complex formed at low temperature does not react below −30 °C and the consumed $[Ag(Br_2AsBr)_2]^+$ shifted the equilibrium of the reaction completely to the side of the dismutation products.
60 The energies of the formation of $EX_2^+$ cations were assessed considering all the species to be in solution (solvated). Additionally, we performed an estimation of the $EX_2^+$ formation in a suitable Born–Haber cycle including the sublimation enthalpies of $EX_3$. The obtained "new" values of the $\Delta G°(CH_2Cl_2)$ of formation of $EX_2^+$, however, differ only very slightly and do not account for the differing behavior of $EX_2^+$ cations (see ESI†).
61 G. Oddo and U. Giachery, *Gazz. Chim. Ital.*, 1924, **53**, 56.
62 P. G. Patfrnosto, *Rev. Facultad Cienc. Quim. (Univ. La Plata)*, 1930, **7**, 43–46.
63 J. C. Bailar, Jr., *Inorg. Synth.*, 1939, **35**, 103–104.
64 R. Ahlrichs, M. Bär, M. Häser, H. Horn and C. Kölmel, *Chem. Phys. Lett.*, 1989, **162**, 165.
65 M. v. Arnim and R. Ahlrichs, *J. Chem. Phys.*, 1999, **111**, 9183.
66 A. D. Becke, *Phys. Rev. A: At. Mol. Opt. Phys.*, 1988, **38**, 3098–3100.
67 K. Eichkorn, O. Treutler, H. Oehm, M. Haeser and R. Ahlrichs, *Chem. Phys. Lett.*, 1995, **242**, 652–660.
68 J. C. Slater, *Phys. Rev.*, 1951, **81**, 385–390.
69 S. H. Vosko, L. Wilk and M. Nusair, *Can. J. Phys.*, 1980, **58**, 1200–1211.
70 J. P. Perdew, *Phys. Rev. B*, 1986, **33**, 8822.
71 A. Klamt and G. Schürmann, *J. Chem. Soc., Perkin. Trans.*, 1993, **2**, 799.
72 Thermal and entropic contributions to the enthalpy and free energy were obtained with TURBOMOLE software package with an exception of $Ag^+$ for which the above contribution were calculated with Gaussian98W at the semiempirical PM3 level.